

Subphthalocyanine Triimides: Solution Processable Bowl-Shaped Acceptors for Bulk Heterojunction Solar Cells

Xiaoshuai Huang,[†] Ming Hu,[†] Xiaohong Zhao,[†] Chao Li,[†] Zhongyi Yuan,^{*,†,‡,§} Xia Liu,[†] Chunsheng Cai,[†] Youdi Zhang,^{†,‡,§} Yu Hu,[†] and Yiwang Chen^{*,†,‡,§}

[†]College of Chemistry and [‡]Institute of Polymers and Energy Chemistry, Nanchang University, 999 Xuefu Avenue, Nanchang 330031, China

Supporting Information

ABSTRACT: Ten subphthalocyanine triimides (SubPcTI) with different substituents at imide sites and B atoms were designed and synthesized. These compounds with low-lying lowest unoccupied molecular orbital energy levels (from -3.91 to -3.98 eV), strong absorption in the range of 450–650 nm, and adjustable solubility are expected to be excellent electron acceptors. Non-fullerene bulk heterojunction organic solar cells based on acceptor **8c** showed power conversion efficiency of 4.92%, which is the highest value among subphthalocyanine derivatives.

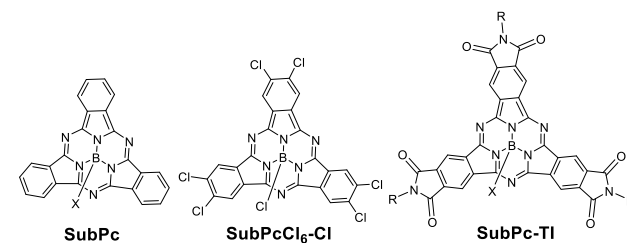
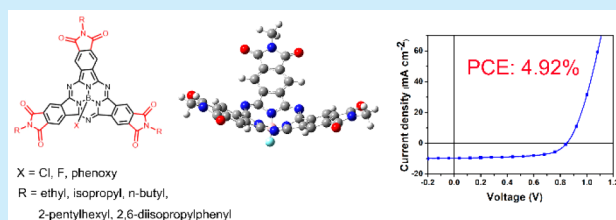


Figure 1. Structures of SubPc, SubPcCl₆-Cl, and SubPcTI.

Bulk heterojunction organic solar cells (BHJOSCs) with advantages of low-cost solution processing, light weight, and charming flexibility have attracted great attention in the past decade.¹ Compared to their high efficiency and rich organic donor counterparts, high-performance electron acceptors are scarce. Despite their weak visible absorption, high cost, and difficult modification, fullerene derivatives such as PC₇₁BM and PC₆₁BM are dominant electron acceptors for long time.²

Non-fullerene acceptors rise rapidly in the past several years. Small-molecule acceptors with well-defined structures, high purity, and tunable absorption have displayed promising performance in BHJOSCs.³ Many BHJOSCs with small-molecule acceptors showed power conversion efficiency (PCE) higher than 10%.⁴ However, these excellent acceptors belong to either perylene diimides (PDI) family or 3,9-bis(2-methylene-(3-(1,1-dicyanomethylene)-indanone))-5,5,11,11-tetrakis(4-hexylphenyl)-dithieno[2,3-d:2',3'-d']-s-indaceno[1,2-b:5,6-b']dithiophene (ITIC) derivatives (structures are in Figure S1).⁵ New acceptor chromophores with excellent performance are desired badly in the field of organic solar cells, because acceptors with different structures, absorption, and crystallinity are required to match with diverse donors, with which matched energy levels, complementary absorption, and suitable phase separation can be coordinated for high-performance devices.⁶

Subphthalocyanine (SubPc, Figure 1) derivatives with bowl-shaped structures have drawn considerable attention in photovoltaic area, due to their strong visible absorption and high carrier mobility.⁷ Three-dimensional structure could reduce serious aggregation in planar conjugated molecules such as PDIs, which is favorable for proper morphology in BHJOSCs. Unsubstituted SubPc with relatively high lowest

unoccupied molecular orbital (LUMO) energy levels ca. -3.5 eV was usually used as donor in organic solar cells.⁸ In addition, SubPcs without substituents show poor solubility, which makes synthesis and solution process difficult. Jones et al.⁹ demonstrated the single-heterojunction organic solar cells with tetracene and SubPc, and a PCE of 2.9% was reached. Paul et al.¹⁰ optimized the SubPc-based bilayer solar cells and obtained a PCE of 4.69%; when fabricating a three-layer device with SubPc, SubNc, and thiophene oligomer, a PCE of 8.4% was got, which is a record efficiency for solar cells based on SubPc derivatives. However, the purification of lightly soluble SubPc is hard, and complicated vapor deposition under fine vacuum and high temperature is necessary.

To transform SubPc into soluble acceptors, some efforts have been done in the past several years. Paul et al.¹¹ firstly introduced F and Cl atoms to peripheral phenyl rings. Halogenated SubPcs with enhanced solubility and lowered LUMO energy levels could be used as solution processable acceptors in BHJOSCs, and the highest PCE of 2.68% was

Received: March 31, 2019

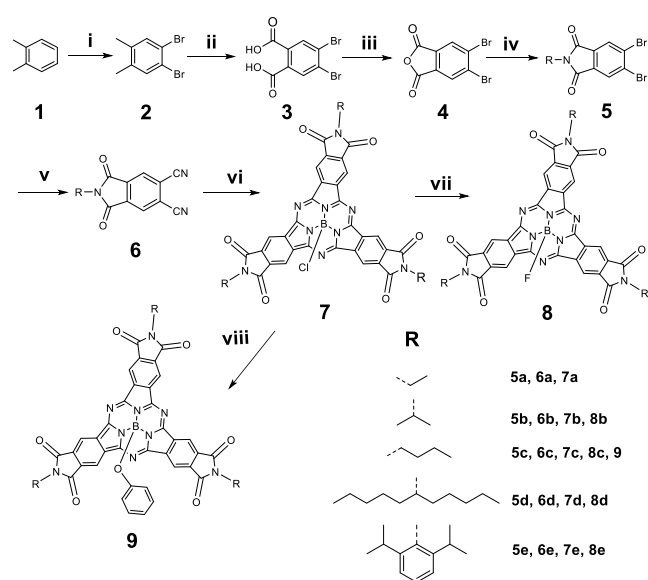
obtained. Recently, Duan et al.¹² optimized non-fullerene BHJOSCs based on SubPcCl₆-Cl and obtained a PCE of 4.0%. SubPc was also used as a building block to construct acceptors. For example, S-SubPc-PDI composed of a SubPc and three PDIs (Figure S2a) showed PCE of 4.53%;¹³ STIC with SubPc and three 2-(3-oxo-2,3-dihydroinden-1-ylidene)-malononitrile (IC) parts (Figure S2b) demonstrated PCE of 4.69%.¹⁴

Imide groups with strong electron-withdrawing property and high stability have been proved to be excellent building blocks in semiconductors.¹⁵ Perylene diimides and naphthalene diimides derivatives were representative star molecules and showed outstanding performance as photovoltaic materials.¹⁶ Herein, three imide groups were fused with SubPc core, and 10 related compounds (SubPcTI, Figure 1) with different substituents at B atoms and imide sites were synthesized. The LUMO energy level of SubPcTI was lowered by 0.35–0.42 eV, and the solubility could be adjusted by alkyl groups at N-terminals. Four of them with suitable solubility were used as acceptors to fabricate BHJOSCs, and the maximum PCE was up to 4.92%, which is the highest efficiency among SubPc-based BHJOSCs.

Since side chains have significant influence on the solubility, mobility, and phase separation of organic acceptors,¹⁷ five different groups at imide positions were adopted in this work. F, Cl, and phenoxy groups at B atom were used to study their effect on absorption, energy levels, and photovoltaic performance.

As shown in Scheme 1, target compounds were synthesized from commercially available *o*-xylene in six or seven steps. Three known compounds 4,5-dibromo-*o*-xylene (2), 4,5-dibromo-*o*-phthalic acid (3), and 4,5-dibromophthalic anhydride (4) were obtained according to literature methods.¹⁸

Scheme 1. Synthetic Route of 7a–7e, 8b–8e, and 9^a



^a(i) I₂, Br₂, 0 °C, 4 h, 77%; (ii) KMnO₄, H₂O, HCl, 140 °C, 7 h, 80%; (iii) 230 °C, 3 h, 97%; (iv) for 5a–5e, acetic acid, corresponding amine, 130 °C, 6 h, 77–88%; (v) for 6a–6e, KI, CuCN, dimethylformamide, 170 °C, 5 h, 63–70%; (vi) for 7a–7e, BCl₃, *p*-xylene, 170 °C, 30 min, 46–55%; (vii) for 8b–8e, AgBF₄, toluene, 30 °C, 7 h, 68–76%; (viii) for 9, phenol, pyridine, toluene, 140 °C, 15 h, 47%.

Dehydration of 3 was performed in acetic anhydride in the literature, while it was heating to 230 °C in this work, which is much simpler for subsequent purification.

Intermediates 4,5-dibromophthalic imides (5a–5e) with different side chains were synthesized by condensation of 4 with corresponding amines in acetic acid in yield of 77–88%. Compounds 5a–5e reacted with CuCN in the presence of KI to afford 4,5-dicyanophthalic imides (6a–6e) in yield of 63–70%, while a more complicated catalyst Pd(PPh₃)₄ was used instead of KI for this kind of reaction in the literature.¹⁹ Compounds 7a–7e were synthesized by cyclization reaction of 6a–6e with BCl₃ in refluxed *p*-xylene in yield of 46–55%.²⁰ Excess BCl₃ and high concentrations of substrates are essential; otherwise, low yield and difficult purification will appear. Compounds 8b–8e were obtained by substitution reaction of 7b–7e with AgBF₄ in toluene.²¹

Substitution reaction of 7c with phenol in refluxed toluene afforded 9 in yield of 47%. Pyridine is necessary. It could complex with acid produced in the reaction, which facilitated the substitution reaction.

All the new compounds 5a–5e, 6a–6e, 7a–7e, 8b–8e, and 9 were characterized clearly by ¹H NMR, ¹³C NMR, and high-resolution mass spectrometry (HRMS). Compounds 7c, 7d, 8c, and 8d with *n*-butyl or 2-pentylhexyl side chains are well-soluble in solvents such as chlorobenzene, chloroform, and toluene, with solubility higher than 20 mg/mL, which makes them solution-processable. The rest of the compounds show limited solubility in organic solvent; their solubility is less than 8 mg/mL in chlorobenzene.

The absorption profiles of these compounds in CH₂Cl₂ and solid state were shown in Figure 2, and corresponding optical

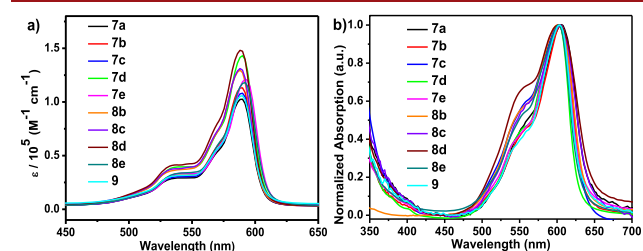


Figure 2. Absorption of SubPcTIs in (a) CH₂Cl₂ (1 × 10^{−5} M) and (b) solid state.

data were summarized in Table 1. All of them with a similar solution profile show strong absorption in the range of 450–650 nm, which indicates that there is little electronic effect of different substituents on the conjugated core. The maximum absorption coefficient of 8d located at 588 nm is up to 148 000 M^{−1} cm^{−1}. Compounds 8b, 8c, and 8e with different side chains show different maximum coefficients because of their different aggregation in solution, as is confirmed in literature.²³ Absorptions of 7a–7e also have the similar phenomenon. Compared to unsubstituted SubPc, introduction of three imide groups causes the solution absorption to red-shift by 20–30 nm (Figure S3a), indicating effective electron communication between imide and SubPc core. Solution absorption in toluene and tetrahydrofuran (THF) were also measured, which produced similar results as those in CH₂Cl₂ (Figure S3b,c). The maximum solid absorption red-shifts by 14–16 nm compared with their corresponding solution results, and absorption edge in solid state also red-shifts by 25–30 nm, indicating strong intermolecular aggregation in solid state.

Table 1. Optical and Electrochemical Data of All SubPcTIs

	λ_{\max}^a (nm)	ϵ ($1 \times 10^3 \text{ M}^{-1} \text{ cm}^{-1}$)	λ_{\max}^b (nm)	Φ_f^c (%)	$\tau^{d,e}$ (ns)	$E_g^{\text{opt } e}$ (eV)	LUMO ^f (eV)
7a	590	102	604	14.3	3.29	1.94	-3.98
7b	590	113	604	15.4	3.31	1.94	-3.93
7c	590	108	602	13.8	3.38	1.94	-3.98
7d	590	143	600	14.3	3.40	1.94	-3.95
7e	592	121	602	15.0	3.36	1.93	-3.93
8b	588	129	602	10.5	2.34	1.93	-3.93
8c	588	131	604	10.1	2.34	1.93	-3.91
8d	588	148	602	9.1	2.35	1.92	-3.94
8e	592	118	602	10.2	2.34	1.93	-3.93
9	592	105	604	11.8	3.07	1.92	-3.96

^aMaximum absorption in CH_2Cl_2 . ^bMaximum absorption in film. ^cFluorescence quantum yield was determined with the standard *N,N'*-di(2,6-isopropylphenyl)-perylene diimides ($\Phi_f = 1$).²² ^dFluorescence lifetime was measured in CH_2Cl_2 . ^eEstimated based on the film absorption onset. ^fMeasured by cyclic voltammetry.

These compounds with optical band gaps in the range of 1.92–1.94 eV belong to moderate bandgap semiconductors.

Emission spectra of these compounds in CH_2Cl_2 were shown in Figure S4, and corresponding data were summarized in Table 1. SubPcTI derivatives with quantum yield of 9.1–15.4% inherit fluorescence characters of SubPc family.^{7b,24} Their emission with peaks located around 610 nm are with Stokes shifts nearby 20 nm.²⁵ The fluorescence-decayed curves were shown in Figure S5, and all the chlorinated compounds 7a–7e with lifetimes of 3.29–3.40 ns are obviously higher than those fluorinated compounds 8b–8e (2.34–2.35 ns), and the reason may be heavy-atom effect of Cl.^{7b} The fluorescence quantum yield of 7a–7e is in the small range of 13.8–15.4%, because of their same parent chromophore, and the little difference is derived from their different aggregation caused by different side chains.

Cyclic voltammetry (CV) measurements (Figure S6) were employed to study their electrochemical properties. All these acceptors showed one semi-reversible reduction peak, indicating their ability to accept at least one electron. Their LUMO energy levels were calculated in the range from -3.91 to -3.98 eV (Table 1), based on the assumption that the energy level of Fc/Fc^+ is 4.8 eV relative to vacuum.²⁶ Above energy levels could match with many donors in BHJOSCs. Compared to parent SubPc, introduction of imide groups lowered LUMO energy levels by 0.35–0.42 eV, due to their strong electron-withdrawing properties.²⁷

Geometries of aromatic cores of these acceptors were optimized with Gaussian 09 program, density functional theory (DFT) method, with basic set of B3LYP/6-311G (d, p).²⁸ Their absorption and band gaps were also calculated. As shown in Figure S7, all these acceptors show bowl-shaped structures. Unlike traditional planar conjugated molecules, rigid three-dimensional structures could cause special molecular packing and electron-transporting properties. Theoretical band gaps of these compounds are 1.71 eV, close to experimental results of 1.92–1.94 eV. Calculated maximum absorption located at 569–573 nm is also near experimental ones (588–592 nm). The accordance of calculated and experimental results confirms the reliability of theoretical method in this study.

An inverted device structure of indium tin oxide (ITO)/ZnO (30 nm)/donor:acceptor/ MoO_3 (7 nm)/Ag (100 nm) was used in BHJOSCs. Donor polymers PBDB-T-SF, PM6, PM7, and PBDB-T-S with matched energy levels and complementary absorption were selected to make solar cells; their structures, energy levels, and absorption were shown in

Figure S8. Photovoltaic results indicated that PM6 performed best with these acceptors (Table S1).

The optimized weight ratio of donor:acceptor was 1:1, as shown in Table S2. Solvent additives 1,8-diiodooctane (DIO), *N*-methyl pyrrolidone (NMP), 1-chloronaphthalene (CN), and 1,2-diphenoxyethane (DPE) could improve device performance, and addition of 0.5% DIO performed best (Table S3). The optimized thickness of active layers was ~90 nm, as determined by atomic force microscopy (AFM; Figure 4).

The current density–voltage (*J*–*V*) curves of devices based on PM6:SubPcTI were illustrated in Figure 3a. Their

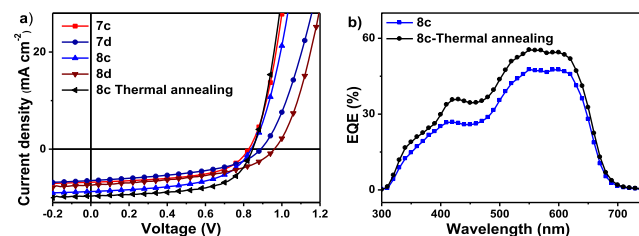


Figure 3. (a) *J*–*V* curves and (b) EQE spectra of solar cells based on PM6:8c.

Table 2. Device Parameters of PM6:SubPcTI Solar Cells

	cond	V_{oc} (V)	J_{sc} (mA/cm^2)	FF (%)	PCE ^a (%)
8c	w/o	0.88	7.00	52.96	(3.09 ± 0.15) 3.24
	DIO	0.84	9.23	52.36	(3.96 ± 0.12) 4.08
	DIO/TA	0.84	9.69	59.92	(4.78 ± 0.14) 4.92
7c	DIO/TA	0.82	7.19	53.09	(2.98 ± 0.17) 3.15
7d	DIO/TA	0.89	6.4	46.26	(2.51 ± 0.16) 2.67
8d	DIO/TA	0.96	7.44	47.12	(3.18 ± 0.19) 3.37

^aThe efficiency value was calculated from 10 devices.

corresponding parameters were summarized in Table 2. Acceptor 8c gave the highest PCE of 4.92%, with V_{oc} of 0.84 V, J_{sc} of 9.69 mA/cm^2 , and the fill factor (FF) of 59.92%. The addition of 0.5% DIO improved PCE from 3.24% to 4.08%. After thermal annealing (TA) at 100 °C for 10 min, the PCE raised to 4.92%.

The external quantum efficiency (EQE) spectra of solar cells based on 8c was shown in Figure 3b. They exhibit broad

photoresponse in the range from 300 to 700 nm, which is contributed by both donor and acceptor. The maximal EQE is 57% with the spectra peak at 550 nm. The EQE spectra of the other acceptors were shown in Figure S10.

The charge mobility of the pure acceptor and SubPcTI:PM6 blend films was evaluated by space-charge limited current (SCLC) method.²⁹ As shown in Table S5 and Figure S11, the electron mobility (μ_e) of the pure films was calculated to be on the magnitude order of $1 \times 10^{-5} \text{ cm}^2 \text{ V}^{-1} \text{ s}^{-1}$; the blended films showed similar μ_e , while their hole mobility (μ_h) was $\sim 1 \times 10^{-4} \text{ cm}^2 \text{ V}^{-1} \text{ s}^{-1}$. Blend films have relatively balanced carrier mobility with μ_h/μ_e of 9.91–19.72. These results demonstrate the four acceptors have good charge-transporting properties for photovoltaic applications.

AFM and transmission electron microscopy (TEM) were employed to investigate the morphology of active layers. As shown in Figure 4, PM6:7c and PM6:8c blend films show

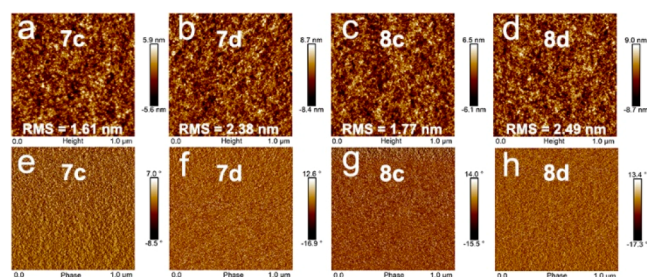


Figure 4. (a–d) AFM height and (e–h) phase images (scale bar: 1.0 μm) of optimum blend films.

small root-mean-square (RMS) roughness of 1.61 and 1.77 nm, indicating their good compatibility with the donor, which led to the higher FF in BHJOSCs. Combining with TEM images (Figure S12), the blend film of PM6:8c showed appropriate domain sizes in nanoscale phase separation. Proper phase separation and domain size were beneficial for exciton separation and charge transport, which contributes to the high J_{sc} , FF, and PCE.

In summary, introduction of imide groups to SubPc was proved to be an effective strategy to construct organic semiconductors. SubPcTI with LUMO energy levels ca. -3.95 eV , adjustable solubility, and strong visible absorption is an excellent chromophore for electron acceptors. Different substituents at imide sites or B atoms showed significant influence on the solubility, mobility, and photovoltaic performance of these acceptors. More functional derivatives deriving from this interesting chromophore deserve intensive investigation, to improve their promising applications in organic solar cells.

ASSOCIATED CONTENT

Supporting Information

The Supporting Information is available free of charge on the ACS Publications website at DOI: 10.1021/acs.orglett.9b01130.

Synthesis and characterization, UV–vis and fluorescence absorption spectra, DFT calculations, cyclic voltammetry, optimization of photovoltaic applications, TEM images, and NMR spectra (PDF)

AUTHOR INFORMATION

Corresponding Authors

*E-mail: yuan@ncu.edu.cn. (Z.-y.Y.)

*E-mail: ywchen@ncu.edu.cn. (Y.-w.C.)

ORCID

Zhongyi Yuan: 0000-0002-8796-4106

Yiwang Chen: 0000-0003-4709-7623

Notes

The authors declare no competing financial interest.

ACKNOWLEDGMENTS

The work was supported by grants from the National Natural Science Foundation of China (Nos. 21562031, 51863012, 51833004, and 51425304) and from the Natural Science Foundation of Jiangxi Province in China (Nos. 20171ACB21012 and 2018ACB21022).

REFERENCES

- (1) (a) Zhang, G.; Zhao, J.; Chow, P. C. Y.; Jiang, K.; Zhang, J.; Zhu, Z.; Zhang, J.; Huang, F.; Yan, H. *Chem. Rev.* **2018**, *118*, 3447–3507. (b) Collins, S. D.; Ran, N. A.; Heiber, M. C.; Nguyen, T.-Q. *Adv. Energy Mater.* **2017**, *7*, 1602242. (c) Liu, F.; Zhou, Z.; Zhang, C.; Vergote, T.; Fan, H.; Liu, F.; Zhu, X. *J. Am. Chem. Soc.* **2016**, *138*, 15523–15526. (d) Li, S.; Liu, W.; Shi, M.; Mai, J.; Lau, T.-K.; Wan, J.; Lu, X.; Li, C.-Z.; Chen, H. *Energy Environ. Sci.* **2016**, *9*, 604–610.
- (2) (a) Cai, C.; Wan, J.; Zhang, Y.; Yuan, Z.; Huang, Q.; Xu, G.; Hu, Y.; Zhao, X.; Chen, Y. *J. Polym. Sci., Part A: Polym. Chem.* **2018**, *56*, 116–124. (b) Yuan, Z.; Li, J.; Xiao, Y.; Li, Z.; Qian, X. *J. Org. Chem.* **2010**, *75*, 3007–3016. (c) Kan, B.; Feng, H.; Wan, X.; Liu, F.; Ke, X.; Wang, Y.; Wang, Y.; Zhang, H.; Li, C.; Hou, J.; Chen, Y. *J. Am. Chem. Soc.* **2017**, *139*, 4929–4934.
- (3) (a) Lin, K.; Xie, B.; Wang, Z.; Xie, R.; Huang, Y.; Duan, C.; Huang, F.; Cao, Y. *Org. Electron.* **2018**, *52*, 42–50. (b) Anthony, J. E.; Facchetti, A.; Heeney, M.; Marder, S. R.; Zhan, X. *Adv. Mater.* **2010**, *22*, 3876–3892.
- (4) (a) Fei, Z.; Eisner, F. D.; Jiao, X.; Azzouzi, M.; Rohr, J. A.; Han, Y.; Shahid, M.; Chesman, A. S. R.; Easton, C. D.; McNeill, C. R.; Anthopoulos, T. D.; Nelson, J.; Heeney, M. *Adv. Mater.* **2018**, *30*, 1705209. (b) Zhang, H.; Yao, H.; Hou, J.; Zhu, J.; Zhang, J.; Li, W.; Yu, R.; Gao, B.; Zhang, S.; Hou, J. *Adv. Mater.* **2018**, *30*, 1800613.
- (5) (a) Lu, Z.; Jiang, B.; Zhang, X.; Tang, A.; Zhan, C.; Yao, J. *Chem. Mater.* **2014**, *26*, 2907–2914. (b) Wang, J.; Wang, W.; Wang, X.; Wu, Y.; Zhang, Q.; Yan, C.; Ma, W.; You, W.; Zhan, X. *Adv. Mater.* **2017**, *29*, 1702125.
- (6) Chen, W.; Zhang, Q. *J. Mater. Chem. C* **2017**, *5*, 1275–1302.
- (7) (a) Jin, F.; Chu, B.; Li, W.; Su, Z.; Yan, X.; Wang, J.; Li, R.; Zhao, B.; Zhang, T.; Gao, Y.; Lee, C. S.; Wu, H.; Hou, F.; Lin, T.; Song, Q. *Org. Electron.* **2014**, *15*, 3756–3760. (b) Claessens, C. G.; Gonzalez-Rodriguez, D.; Rodriguez-Morgade, M. S.; Medina, A.; Torres, T. *Chem. Rev.* **2014**, *114*, 2192–2277. (c) Beaumont, N.; Castrucci, J. S.; Sullivan, P.; Morse, G. E.; Paton, A. S.; Lu, Z.-H.; Bender, T. P.; Jones, T. S. *J. Phys. Chem. C* **2014**, *118*, 14813–14823.
- (8) (a) Lin, C.-F.; Nichols, V. M.; Cheng, Y.-C.; Bardeen, C. J.; Wei, M.-K.; Liu, S.-W.; Lee, C.-C.; Su, W.-C.; Chiu, T.-L.; Han, H.-C.; Chen, L.-C.; Chen, C.-T.; Lee, J.-H. *Sol. Energy Mater. Sol. Cells* **2014**, *122*, 264–270. (b) Mutolo, K. L.; Mayo, E. I.; Rand, B. P.; Forrest, S. R.; Thompson, M. E. *J. Am. Chem. Soc.* **2006**, *128*, 8108–8109.
- (9) Beaumont, N.; Cho, S. W.; Sullivan, P.; Newby, D.; Smith, K. E.; Jones, T. S. *Adv. Funct. Mater.* **2012**, *22*, 561–566.
- (10) Cnops, K.; Rand, B. P.; Cheyns, D.; Verreert, B.; Empl, M. A.; Heremans, P. *Nat. Commun.* **2014**, *5*, 3406.
- (11) Sullivan, P.; Duraud, A.; Hancox, I.; Beaumont, N.; Mirri, G.; Tucker, J. H. R.; Hatton, R. A.; Shipman, M.; Jones, T. S. *Adv. Energy Mater.* **2011**, *1*, 352–355.

- (12) Duan, C.; Zango, G.; Garcia Iglesias, M.; Colberts, F. J.; Wienk, M. M.; Martinez-Diaz, M. V.; Janssen, R. A.; Torres, T. *Angew. Chem., Int. Ed.* **2017**, *56*, 148–152.
- (13) Hang, H.; Zhang, Z.; Wu, X.; Chen, Y.; Li, H.; Wang, W.; Tong, H.; Wang, L. *J. Mater. Chem. C* **2018**, *6*, 7141–7148.
- (14) Hang, H.; Wu, X.; Xu, Q.; Chen, Y.; Li, H.; Wang, W.; Tong, H.; Wang, L. *Dyes Pigm.* **2019**, *160*, 243–251.
- (15) Wu, Q.; Zhao, D.; Schneider, A. M.; Chen, W.; Yu, L. *J. Am. Chem. Soc.* **2016**, *138*, 7248–7251.
- (16) (a) Zhong, Y.; Trinh, M. T.; Chen, R.; Purdum, G. E.; Khlyabich, P. P.; Sezen, M.; Oh, S.; Zhu, H.; Fowler, B.; Zhang, B.; Wang, W.; Nam, C. Y.; Sfeir, M. Y.; Black, C. T.; Steigerwald, M. L.; Loo, Y. L.; Ng, F.; Zhu, X. Y.; Nuckolls, C. *Nat. Commun.* **2015**, *6*, 8242. (b) Yi, J.; Wang, Y.; Luo, Q.; Lin, Y.; Tan, H.; Wang, H.; Ma, C. *Q. Chem. Commun.* **2016**, *52*, 1649–1652.
- (17) Lian, X.; Zhang, L.; Hu, Y.; Zhang, Y.; Yuan, Z.; Zhou, W.; Zhao, X.; Chen, Y. *Org. Electron.* **2017**, *47*, 72–78.
- (18) (a) He, N.; Chen, Y.; Doyle, J.; Liu, Y.; Blau, W. J. *Dyes Pigm.* **2008**, *76*, 569–573. (b) Wang, X.; Zhang, Y.; Sun, X.; Bian, Y.; Ma, C.; Jiang, J. *Inorg. Chem.* **2007**, *46*, 7136–7141.
- (19) Gonidec, M.; Amabilino, D. B.; et al. *Dalton Trans* **2012**, *41*, 13632–13639.
- (20) Giribabu, L.; Vijay Kumar, C.; Surendar, A.; Gopal Reddy, V.; Chandrasekharam, M.; Yella Reddy, P. *Synth. Commun.* **2007**, *37*, 4141–4147.
- (21) Guilleme, J.; Gonzalez-Rodriguez, D.; Torres, T. *Angew. Chem.* **2011**, *123*, 3568–3571.
- (22) Wurthner, F. *Chem. Commun.* **2004**, 1564–1579.
- (23) Li, Y.; Gao, J.; Di Motta, S.; Negri, F.; Wang, Z. *J. Am. Chem. Soc.* **2010**, *132*, 4208–4213.
- (24) Shimizu, S.; Miura, A.; Khene, S.; Nyokong, T.; Kobayashi, N. *J. Am. Chem. Soc.* **2011**, *133*, 17322–17328.
- (25) Turrise, R.; Sanguineti, A.; Sassi, M.; Savoie, B.; Takai, A.; Patriarca, G. E.; Salamone, M. M.; Ruffo, R.; Vaccaro, G.; Meinardi, F.; Marks, T. J.; Facchetti, A.; Beverina, L. *J. Mater. Chem. A* **2015**, *3*, 8045–8054.
- (26) Xia, D.; Wu, Y.; Wang, Q.; Zhang, A.; Li, C.; Lin, Y.; Colberts, F. J. M.; van Franeker, J. J.; Janssen, R. A. J.; Zhan, X.; Hu, W.; Tang, Z.; Ma, W.; Li, W. *Macromolecules* **2016**, *49*, 6445–6454.
- (27) Zhu, G.; Zhang, Y.; Hu, Y.; Zhao, X.; Yuan, Z.; Chen, Y. *J. Polym. Sci., Part A: Polym. Chem.* **2018**, *56*, 276–281.
- (28) Zhao, X.; Xiong, Y.; Ma, J.; Yuan, Z. *J. Phys. Chem. A* **2016**, *120*, 7554–7560.
- (29) Zhang, Y.; Guo, X.; Su, W.; Guo, B.; Xu, Z.; Zhang, M.; Li, Y. *Org. Electron.* **2017**, *41*, 49–55.